

Nicotine-induced miR-21-3p promotes chemoresistance in lung cancer by negatively regulating FOXO3a

YONG-QING ZHANG, RUI-LIN CHEN, LI-QUN SHANG and SHU-MEI YANG

Department of Respiratory and Critical Care Medicine,
Shaanxi Provincial People's Hospital, Xi'an, Shaanxi 710068, P.R. China

Received January 6, 2021; Accepted October 1, 2021

DOI: 10.3892/ol.2022.13380

Abstract. Lung cancer is the leading cause of cancer-related mortality worldwide and cigarette smoking is reported to contribute to the lung cancer-related mortality. The present study aimed to investigate the molecular mechanism underlying nicotine-induced chemoresistance in lung cancer. The expression of microRNA (miR)-21-3p and its predicted target FOXO3a in lung cancer cells was detected via reverse transcription-quantitative PCR, in the presence or absence of nicotine. The regulatory effect of miR-21-3p and FOXO3a on lung cancer cell proliferation and apoptosis induced by docetaxel or cisplatin treatment was evaluated by performing Cell Counting Kit-8 and Annexin V/PI staining assays, respectively. The interaction between miR-21-3p and FOXO3a was analyzed by performing luciferase reporter assays and western blotting. FOXO3a overexpression rescue experiments were conducted *in vitro* and *in vivo* using a xenograft mouse model to assess the function of miR-21-3p/FOXO3a in lung cancer. Nicotine induced miR-21-3p expression in lung cancer cells in a dose-dependent manner. miR-21-3p downregulated FOXO3a expression by directly binding to the 3'-untranslated region of FOXO3a. Moreover, miR-21-3p knockdown sensitized lung cancer cells to docetaxel or cisplatin treatment. Mechanistically, FOXO3a was predicted as a direct target of miR-21-3p. FOXO3a overexpression promoted the chemosensitivity of lung cancer cells to docetaxel or cisplatin treatment. Furthermore, FOXO3a overexpression antagonized the regulatory function of miR-21-3p on docetaxel- or cisplatin-treated lung cancer cells. In the docetaxel- or cisplatin-treated lung cancer xenograft mouse model, miR-21-3p promoted chemoresistance via negatively regulating FOXO3a. Therefore, the present study demonstrated that nicotine-induced miR-21-3p promoted chemoresistance to docetaxel or cisplatin treatment

via negatively regulating FOXO3a, which may serve as a novel therapeutic strategy for the treatment of patients with chemoresistant lung cancer.

Introduction

Cigarette smoking imposes multiple complex impacts on human health and systemically affects all organs to variable extents (1). Cigarette smoke contains >60 harmful chemicals, including polycyclic hydrocarbons, tar, phenol and nitrosamine, which are carcinogens that damage the DNA, and carbon monoxide, which attaches to the heme groups and inhibits cytochrome oxidase in the electron transport chain (2). Moreover, cigarette smoking is the most common cause of chronic obstructive pulmonary disease (COPD), and also increases the risk for a variety of malignancies involving major organ systems, including the gastrointestinal, respiratory and genitourinary systems (3). In particular, cigarette smoking accounts for ~90% of lung cancer-related deaths (4). Furthermore, smokeless tobacco and passive smoke inhalation cause nicotine addiction, oral squamous cell carcinoma, lung cancer, respiratory and middle ear infections, and exacerbation of asthma (5). Recent studies have shown that electronic-cigarette smoke (vaping) is associated with the impairment of innate immunity, lung injury due to the disruption of lung lipid homeostasis and potential risk of lung adenocarcinoma (6,7).

Interestingly, cigarette smoking causes persistent changes in the expression of numerous genes in the airway epithelium, regardless of smoking cessation (8,9); however, this long-lasting profound gene signature is not completely understood. Consistent with this biological change, limited data have shown a tenacious alteration of functional microRNAs (miRNA/miR), such as miR-634 and miR-1246, in the respiratory epithelium of healthy smokers (10). Several groups have conducted comprehensive profiling of epigenetic change in smokers: Willinger *et al* (11) identified a smoking-related miRNA/mRNA co-expressed gene network involved in smoking-induced inflammatory processes; and Qian *et al* (12) investigated the pivotal role of the miR-122-5p/ α 2-macroglobulin (A2M)/LINC00987/A2M-antisense RNA 1/LINC0061 network in the pathogenesis of COPD, irrespective of the smoking status. Moreover, a previous study demonstrated that electronic cigarettes, with or without the presence of nicotine,

Correspondence to: Dr Shu-Mei Yang, Department of Respiratory and Critical Care Medicine, Shaanxi Provincial People's Hospital, 256 Youyi West Road, Xi'an, Shaanxi 710068, P.R. China
E-mail: sanpingchen@nwu.edu.cn

Key words: lung cancer, nicotine, chemo-resistance, microRNA-21-3p, FOXO3a

significantly disturbed miRNA regulation in primary human bronchial epithelial cells (13).

Another significant emerging adverse effect of cigarette smoking on human health lies in its induction of chemoresistance in neoplastic cells, as observed in a number of solid tumors, such as glioblastoma, breast cancer, lung cancer, pancreatic cancer, nasopharyngeal carcinoma and bladder cancer (14-16). The underlying mechanisms are not fully understood yet, but accumulating data have shown the multifaceted effects of nicotine on tumor growth. For example, nicotine promotes neural tumor cell proliferation by interfering with the PI3K, EGFR and cytochrome P450 2B1 signaling pathways, and also facilitates tumor invasion by inducing angiogenesis in the tumor microenvironment (17-20). Moreover, nicotine suppresses the expression of miR-296-3p in nasopharyngeal carcinoma cells, leading to upregulated mitogen-activated protein kinase-activated protein kinase 2 protein and subsequent chemoresistance to cisplatin (21). Pharmacodynamically, nicotine reduces the bioavailability of cytochrome-P450-metabolized agents, such as carmustine (14). Therefore, understanding the mechanisms underlying nicotine-induced chemoresistance would guide oncologists on optimal clinical outcomes.

In the present study, miR-21-3p, a novel miRNA, was detected in patients with lung cancer with or without consistent nicotine consumption, and in lung cancer cell lines. Furthermore, the role and mechanism of miR-21-3p underlying nicotine-induced chemoresistance in lung cancer were also evaluated using proliferation and apoptosis analyses. Based on these analyses, the present study aimed to provide a novel therapeutic target for the treatment of nicotine-related chemoresistant lung cancer.

Materials and methods

Patient specimen. A total of 10 paired lung cancer tissues and adjacent tissues (distance from tumor margin, 1 cm) were obtained from patients with lung cancer with (n=5; mean age, 57.2±7.79 years; age range, 45-64 years) or without (n=5; mean age, 56.4±9.45 years; age range, 45-67 years) consistent nicotine consumption at Shaanxi Provincial People's Hospital (Shaanxi, China) between January 2018 to December 2019. The following inclusion criteria were used: i) aged >18 years; ii) diagnosed by biopsy analysis; iii) detailed clinical characteristics recorded; and vi) signed informed consent and agreement term. Patients who also suffered infectious diseases or other types of cancer were excluded from the study. The clinical characteristics of the enrolled patients are summarized in Table I. TNM stage of patients was estimated according to The Eight Edition Lung Cancer Stage Classification (22). All tissues samples were snap frozen in liquid nitrogen and stored at -80°C until further analysis. The patient studies performed in the present study were approved by the Medical Ethics Committee of Shaanxi Provincial People's Hospital (approval no. SXRMY-2019-024). All patients signed informed consent and agreement term.

Cell culture and treatment. Human lung cancer cell lines (A549, NCI-H460, SW900 and NCI-H520) were obtained from American Type Cell Collection. The human bronchial

epithelial cell line (BEAS-2B) was purchased from The Cell Bank of Type Culture Collection of The Chinese Academy of Sciences. All cell lines were cultured in RPMI-1640 (BEAS-2B, SW900 and NCI-H520; Invitrogen; Thermo Fisher Scientific, Inc.) or DMEM (A549 and NCI-H460; Invitrogen; Thermo Fisher Scientific, Inc.) supplemented with 10% FBS (Invitrogen; Thermo Fisher Scientific, Inc.), 100 U/ml penicillin and 100 µg/ml Streptomycin (Sigma-Aldrich; Merck KGaA) at 37°C in a humidified incubator with 5% CO₂. Nicotine, docetaxel and cisplatin were obtained from Sigma-Aldrich (Merck KGaA) and prepared according to the manufacturer's protocol. For nicotine treatment, the cells were treated with nicotine (0, 0.1, 1, 10 or 100 µM) for 24 h and cultured at 37°C; for docetaxel treatment, the cells were treated with different concentrations of docetaxel (1, 10, 100 or 1,000 nM) for 24 h and cultured at 37°C; for cisplatin treatment, cells were treated with different concentrations of cisplatin (0.1, 0.5, 1.0 or 5.0 µM) for 24 h and cultured at 37°C.

Transfection. A549 or NCI-H460 cells were seeded (4×10⁵ cells/well) into 6-well plates overnight. Subsequently, cells were transfected with 50 nM miR-21-3p mimic, 50 nM miR-21-3p inhibitor, 50 nM inhibitor negative control (NC), 50 nM mimic NC, 100 nM pcDNA 3.1-FOXO3a or 100 nM pcDNA 3.1 (negative control for overexpression) using Lipofectamine[®] 3000 (Invitrogen; Thermo Fisher Scientific, Inc.) according to the manufacturer's protocol. Cells were transfected at 37°C for 48 h. At 48 h post-transfection, cells were used for subsequent experiments. miRNA transfection efficiency was confirmed by reverse transcription-quantitative PCR (RT-qPCR), and mRNA transfection efficiency was confirmed by RT-qPCR and western blotting. Specifically, miR-21-3p inhibitor (5'-GCCCAUCGACUGGUGUUG-3'), inhibitor NC (5'-CAGUACUUUUGUGUAGUACAA-3'), miR-21-3p mimic (5'-CAACACCAGUCGAUGGGCUGU-3') and mimic NC (5'-UUCUCCGAACGUGUCACGUUU-3') were purchased from Hanbio Biotechnology Co., Ltd. pcDNA3.1-FOXO3a and pcDNA 3.1 (empty vector NC) were obtained from Shanghai GenePharma Co., Ltd.

RT-qPCR. Total RNA was extracted from tissue or cell samples using the RNeasy Plus Mini Kit (Qiagen GmbH) and 0.2 µg RNA was reverse transcribed into cDNA using SuperScriptase III (Invitrogen; Thermo Fisher Scientific, Inc.) according to the manufacturer's protocol. Subsequently, qPCR was performed using PowerUP SYBR Green master mix (Applied Biosystems; Thermo Fisher Scientific, Inc.) with the following thermocycling conditions: Initial denaturation at 95°C for 10 min, followed by 40 cycles of denaturation at 95°C for 10 sec, annealing at 58°C for 30 sec and elongation at 72°C for 10 sec. The relative expression of miRNA and mRNA was calculated using the 2^{-ΔΔC_q} method (23) and normalized to the internal reference genes U6 and β-actin, respectively. The primer sequences used for qPCR were as follows: miR-21-3p forward, 5'-GCAACACCAGTCGATGGGCTG T-3' with a Universal PCR Reverse Primer (cat. no. B532451; Sangon Biotech Co., Ltd.); U6 forward, 5'-CTCGCTTCG GCAGCACA-3' and reverse, 5'-AACGCTTCACGAATTTGC GT-3'; FOXO3a forward, 5'-ACAAACGGCTCACTCTGT CC-3' and reverse, 5'-CAGTTCCTCATTCTGGACCC-3';

Table I. Clinicopathological features of 10 patients with lung cancer.

Characteristic	Non-smoker, n (%)	Smoker, n (%)
Age, years		
≥60	3 (60)	3 (60)
<60	2 (40)	2 (40)
Sex		
Male	4 (80)	4 (80)
Female	1 (80)	1 (20)
Histology		
Adenocarcinoma	3 (60)	3 (60)
Squamous cell carcinoma	2 (40)	2 (40)
TNM stage		
I+II	4 (80)	3 (60)
III+IV	1 (20)	2 (40)
Lymphatic metastasis		
Positive	1 (20)	2 (40)
Negative	4 (80)	3 (60)
Distant metastasis		
Positive	0 (0)	1 (20)
Negative	5 (100)	4 (80)

protocadherin 19 (PCDH19) forward, 5'-ACTCTTTCAACA GCCAGGGG-3' and reverse, 5'-TGAAGGTGGAGCTGC TCTTG-3'; ATPase Na⁺/K⁺ transporting subunit β1 (ATP1B1) forward, 5'-TGGCATCTTCATCGGAACCAT-3' and reverse, 5'-ATCTGTCTTAATCCTGGCGG-3'; and β-actin forward, 5'-GCTCCGGCATGTGCAA-3' and reverse, 5'-GTCAT TGAGAAAGTGTGGTG-3'. All the primers were designed and synthesized by Sangon Biotech Co., Ltd.

Western blotting. Total protein was isolated from A549 or NC-H460 cells using RIPA buffer (Beyotime Institute of Biotechnology). Protein concentrations were measured using a BCA kit (Pierce; Thermo Fisher Scientific, Inc.). Equal amounts of protein (25 μg) were loaded and separated via 12% SDS-PAGE. Proteins were transferred to PVDF membranes in an AccuRef fast transferring buffer (AccuRef Scientific) and blocked with an AccuRef Blocking Reagent (AccuRef Scientific) at room temperature for 15 min. Subsequently, the membranes were incubated with rabbit monoclonal anti-human FOXO3a (1:1,000; cat. no. 2497S) and β-actin (1:1,000; cat. no. 4970S) primary antibodies (both Cell Signaling Technology, Inc.) at 4°C overnight. After washing three times with PBS, the membranes were incubated with a HRP-conjugated mouse anti-rabbit secondary antibody (1:3,000; cat. no. 7074S; Cell Signaling Technology, Inc.) at room temperature for 1 h. Following a further three washes with PBS, the protein bands were detected using a chemiluminescence kit (Pierce; Thermo Fisher Scientific, Inc.). Protein expression was semi-quantified using ImageJ software (version 1.5; National Institutes of Health) with β-actin as the loading control.

Cell proliferation assay. Transfected A549 or NCI-H460 cells were seeded (2x10³ cells/well) into 96-well plates and then treated different concentrations of docetaxel (1, 10, 100 or 1,000 nM) or cisplatin (0.1, 0.5, 1.0 or 5.0 μM) for 48 h. Subsequently, Cell Counting Kit-8 (CCK-8) reagent (AccuRef Scientific) was added to the cell culture and cells were maintained for 2 h. The absorbance was measured at a wavelength of 490 nm using a spectrophotometer (Molecular Devices, LLC).

Cell apoptosis assay. A549 or NCI-H460 cells treated as indicated for the cell proliferation assay were collected and stained with Annexin V-FITC/PI using an Annexin V-FITC Apoptosis Detection Kit (AccuRef Scientific) according to the manufacturer's protocol. Cell apoptosis was analyzed by flow cytometry and the apoptotic cells were defined as Annexin V⁺/PI⁺ cells using the FACSaria II flow cytometer (BD Biosciences) and analyzed using FlowJo software (version 7; FlowJo LLC).

Luciferase assay. The plasmids of the wild-type (WT) and mutated (MUT) 3'-untranslated region (UTR) of FOXO3a constructed into the pGL3-Luc vector (Promega Corporation) were purchased from Shanghai GeneChem Co., Ltd. For the luciferase assay, 2.0x10⁴ A549 cells were cultured in a 48-well plate overnight and co-transfected with pGL3-WT FOXO3a 3'-UTR (100 nM) or pGL3-MUT FOXO3a 3'-UTR (100 nM) and miR-21-3p mimic (50 nM) or mimic NC (50 nM) using Lipofectamine[®] 3000 (Invitrogen; Thermo Fisher Scientific, Inc.) according to the manufacturer's protocol. The cells were transfected at 37°C for 48 h. At 48 h post-transfection at 37°C, relative luciferase activities were analyzed using a Dual-Glo luciferase system kit (Promega Corporation) according to the manufacturer's protocol with *Renilla* luciferase activity as the normalization control.

Target prediction. To further investigate the mechanism underlying miR-21-3p, the downstream targets of miR-21-3p were predicted using the microT (http://diana.imis.athena-innovation.gr/DianaTools/index.php?r=microT_CDS/index) and miRNA Database (miRDB; <http://mirdb.org/index.html>) databases followed by Venn analysis (version 2.1; <https://bioinfogp.cnb.csic.es/tools/venny/>).

Xenograft tumor model. The present study was performed at Shaanxi Provincial People's Hospital and all experiments were performed in accordance with the Guidelines of the Animal Use and Care Committee of Shaanxi Provincial People's Hospital (Shaanxi, China). The animal experiments performed in the present study were approved by the Institutional Review Board of Shaanxi Provincial People's Hospital (approval no. XJTULAC20181428). A total of 18 male BALB/c nude mice (age, 5 weeks; weight, 20-22 g) were purchased from Beijing Vital River Laboratory Animal Technology Co., Ltd. and maintained in the animal facility at Shaanxi Provincial People's Hospital at room temperature (22±1°C) and 40-60% humidity with 12-h light/dark cycles, and *ad libitum* access to food and water. A total of 2x10⁶ transfected A549 cells in PBS (pcDNA3.1, pcDNA3.1-FOXO3a, and pcDNA3.1-FOXO3a + miR-21-3p mimic) were inoculated into the left flank of BALB/c nude mice to establish the xenograft

tumor model. After inoculation, the mice were intraperitoneally injected with nicotine (0.25 mg/kg body weight) every 3 days until sacrifice. Mice were intraperitoneally injected with 5 mg/kg docetaxel or cisplatin every 7 days. The tumor size was measured every 4 days. For nicotine, docetaxel or cisplatin treatment, an equal volume of DMSO was used as the control treatment. At 17 days after cell inoculation, the mice were anesthetized via intramuscular injection of 50 mg/kg ketamine mixed with 5 mg/kg xylazine. Subsequently, the mice were euthanized by cervical dislocation, and the tumors were extracted and weighed.

Immunohistochemical analysis. After sacrifice, the partial tumor samples were fixed with 4% formaldehyde at 4°C overnight. The tissues were dehydrated with a gradient ethanol solution, transparentized with xylene and paraffin-embedded at 60°C for >6 h. Then, the tissues were cut into 5- μ m slices, deparaffinized at 60°C for 1 h and rehydrated in a gradient ethanol solution. Antigen retrieval was performed in boiled 0.01 M sodium citrate buffer (pH 6.0) in a microwave for three times (3 min per boil) with 5 min intervals. Following this, the slices were incubated with 3% H₂O₂ at room temperature for 5-10 min to block endogenous peroxidase. After washing with PBS three times, the slices were blocked with an AccuRef Blocking Reagent (AccuRef Scientific) at room temperature for 30 min. Subsequently, the slices were incubated with a rabbit anti-mouse Ki-67 antibody (1:200; cat no. ab15580; Abcam) in a humidified incubator at 4°C overnight. After washing three times with PBS, the slices were incubated with a donkey anti-rabbit secondary antibody (1:500; cat. no. ab207999; Abcam) at room temperature for 45 min in a humidified incubator. For visualization, the DAB Substrate Kit (cat. no. ab64238; Abcam) was used according to the manufacturer's protocol, followed by hematoxylin counterstaining at room temperature for 3-5 min. Subsequently, slices were washed with running water for 10 min, dehydrated with ethanol, hyalinized with xylene and mounted with neutral resins (cat. no. E675007; Sangon Biotech Co., Ltd). To quantify Ki-67 staining in the nucleus, the Ki-67⁺ cell rate was estimated by counting the number of Ki-67⁺ cell nuclei per 1,200-1,800 tumor cells in three different fields of views with the greatest staining density under a light microscope (Nikon Corporation). Finally, the average Ki-67⁺ cell rate of each sample was calculated using ImageJ software (version 1.49; National Institutes of Health).

Statistical analysis. Data are presented as the mean \pm SD of at least three independent experiments. Statistical analyses were performed using GraphPad Prism Software (version 8.0.1; GraphPad Software, Inc.). Comparisons between two groups were analyzed using the unpaired Student's t-test. Comparisons among multiple groups were analyzed using one-way ANOVA followed by Tukey's post hoc test. P<0.05 was considered to indicate a statistically significant difference.

Results

Nicotine induces miR-21-3p expression in lung cancer cells. A previous study has indicated that nicotine upregulates miR-21-3p in esophageal cancer cells (24). To observe the effect of nicotine on the expression of miR-21-3p in lung cancer, the expression of miR-21-3p in the lung cancer tissues

of patients with or without consistent nicotine consumption was assessed. The results revealed that the expression of miR-21-3p was significantly increased in tumors compared with that in adjacent normal tissues, and nicotine consumption significantly enhanced miR-21-3p expression in lung tumor tissues (Fig. 1A). Furthermore, the expression of miR-21-3p in the lung cancer cell lines was also determined. The results suggested that miR-21-3p was significantly upregulated in lung cancer cell lines compared with that in the BEAS-2B cell line, and the A549 cell line displayed the most upregulated expression levels, followed by the H460 cell line among the lung cancer cell lines (Fig. 1B). Therefore, human lung cancer A549 or NCI-H460 cell lines were treated with different concentrations of nicotine. As shown in Fig. 1C and D, nicotine displayed a dose-dependent effect on miR-21-3p expression, with significantly upregulated miR-21-3p expression in the 10 and 100 μ M nicotine treatment groups compared with that in the control group. These results indicated that nicotine induced miR-21-3p expression in lung cancer cells in a dose-dependent manner.

miR-21-3p knockdown sensitizes lung cancer cells to docetaxel and cisplatin treatment. To investigate the functional role of miR-21-3p in the chemoresistance of lung cancer cells, miR-21-3p inhibitor was used to knock down miR-21-3p expression in A549 and NCI-H460 cells treated with or without nicotine (Fig. 2A and B). The RT-qPCR results confirmed that miR-21-3p inhibitor significantly decreased the expression of miR-21-3p compared with that in the inhibitor NC group, and nicotine treatment significantly increased miR-21-3p expression levels, reversing miR-21-3p inhibitor-mediated decreases in miR-21-3p expression in both A549 and NCI-H460 cells (Fig. 2A and B).

Cell proliferation was evaluated using the CCK-8 assay. The results demonstrated that miR-21-3p inhibitor significantly decreased cell survival in the presence of docetaxel or cisplatin compared with that in the inhibitor NC group, whereas nicotine treatment significantly attenuated these miR-21-3p inhibitor-induced effects (Fig. 2C-F), suggesting that miR-21-3p mediated the chemoresistance of lung cancer cells and nicotine reversed these effects. Moreover, the function of miR-21-3p in the apoptosis of lung cancer cells induced by the chemotherapeutic drugs docetaxel or cisplatin was assessed. The flow cytometry results demonstrated that miR-21-3p knockdown significantly increased the apoptosis of docetaxel- or cisplatin-treated A549 and NCI-H460 cells compared with the inhibitor NC group, whereas nicotine treatment significantly inhibited this effect (Fig. 2G-J). These results suggested that nicotine might promote the chemoresistance of lung cancer cells via increasing the expression of miR-21-3p, and downregulating miR-21-3p could sensitize lung cancer cells to docetaxel or cisplatin treatment.

FOXO3a is a downstream target of miR-21-3p in lung cancer cells. Bioinformatics analysis was performed using microT and miRDB databases, and PCDH19, ATP1B1 and FOXO3a were predicted as miR-21-3p targets by both tools (Fig. 3A). A549 cells were transfected with the miR-21-3p inhibitor or inhibitor NC, followed by the determination of PCDH19, ATP1B1, and FOXO3a expression via RT-qPCR. No significant alterations in the expression levels of

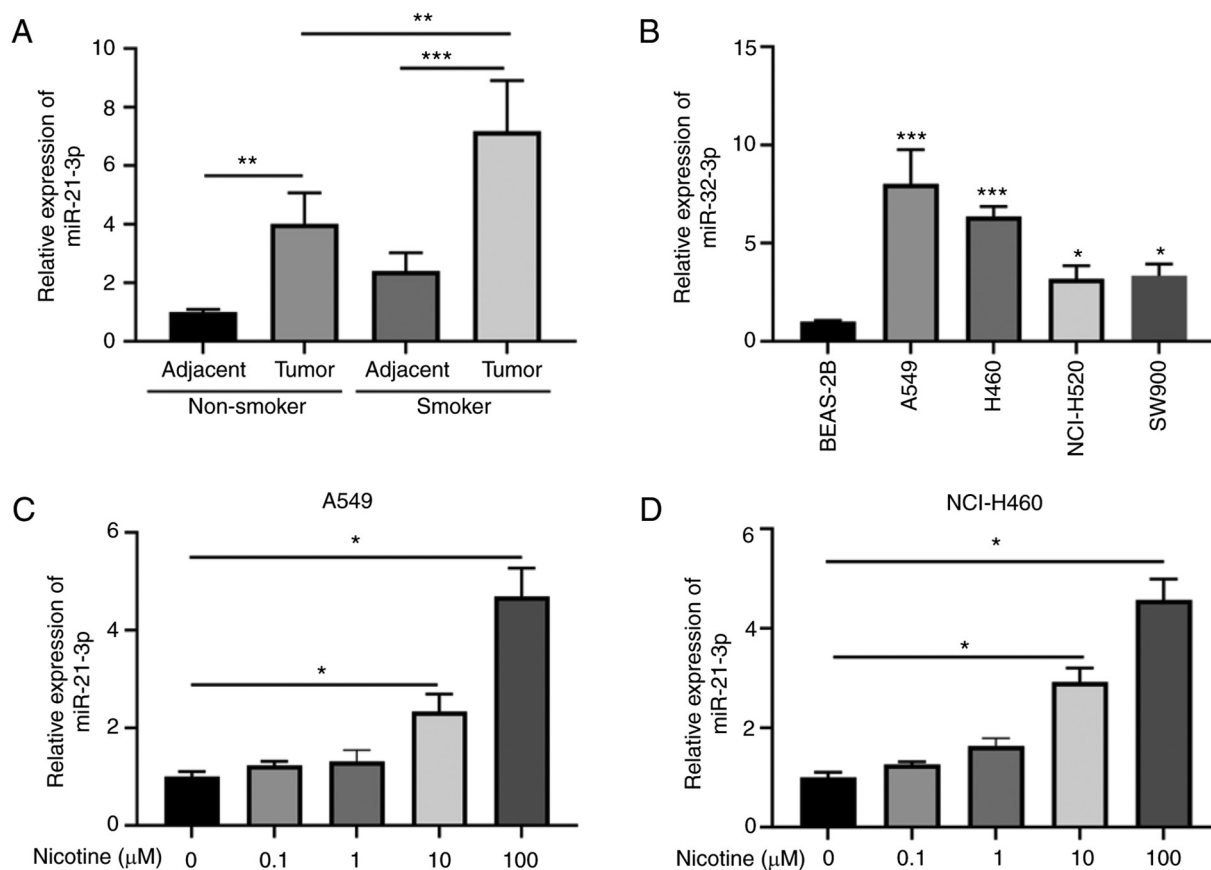


Figure 1. Nicotine induces miR-21-3p expression in lung cancer cells. (A) miR-21-3p expression in lung cancer tissues from patients with or without consistent nicotine consumption was analyzed by RT-qPCR (n=5). (B) miR-21-3p expression in lung cancer cell lines (A549, H460, NCI-H520 and SW900) and the human bronchial epithelial cell line (BEAS-2B) (n=3). (C) A549 or (D) NCI-H460 cells were treated with different concentrations of nicotine (0, 0.1, 1, 10 or 100 μ M) for 24 h. miR-21-3p expression in A549 or NCI-H460 cells was analyzed by RT-qPCR (n=3). Data were presented as mean \pm SD. *P<0.05, **P<0.01 and ***P<0.001 vs. BEAS-2B or as indicated. miR, microRNA; RT-qPCR, reverse transcription-quantitative PCR.

PCDH19 and ATP1B1 were identified, whereas FOXO3a expression was significantly enhanced following miR-21-3p inhibitor transfection compared with following inhibitor NC transfection, indicating that miR-21-3p directly regulated FOXO3a expression (Fig. 3B). A 100% sequence match was identified between miR-21-3p and the 3'-UTR of FOXO3a (Fig. 3C). The luciferase assay was used to evaluate the specific targeting of FOXO3a by miR-21-3p in A549 cells. As expected, miR-21-3p knockdown significantly enhanced the relative luciferase activity of the WT FOXO3a 3'-UTR vector compared with that in cells transfected with inhibitor NC (Fig. 3D). Conversely, miR-21-3p inhibitor did not significantly affect the luciferase activity of the mutated FOXO3a 3'-UTR vector (Fig. 3D). The western blotting results revealed that the expression of the FOXO3a protein was significantly enhanced in A549 and NCI-H460 cells transfected with miR-21-3p inhibitor compared with those transfected with inhibitor NC (Fig. 3E and F). Intriguingly, the mRNA expression of FOXO3a was significantly downregulated in tumor tissues compared with that in adjacent normal tissues, and the downregulation was more obvious in tumor tissues isolated from patients who smoked compared with those in non-smoker patients (Fig. 3G). Moreover, both 10 and 100 μ M nicotine markedly decreased the expression of FOXO3a in A549 and NCI-H460 cells in a dose-dependent manner (Fig. 3H and I). Compared with that in the inhibitor

NC group, miR-21-3p knockdown significantly increased FOXO3a expression, but nicotine treatment significantly inhibited miR-21-3p inhibitor-induced upregulation of FOXO3a in A549 and NCI-H460 cells (Fig. 3J and K). These data indicated that miR-21-3p specifically downregulated FOXO3a expression in lung cancer cells.

miR-21-3p promotes the chemoresistance of lung cancer cells via negatively regulating FOXO3a in vitro. To verify the function of FOXO3a and the interaction between FOXO3a and miR-21-3p in the chemoresistance of lung cancer cells, A549 or NCI-H460 cells were transfected with pcDNA3.1-FOXO3a, miR-21-3p mimic or their corresponding controls. The RT-qPCR results suggested that miR-21-3p overexpression significantly increased the expression of miR-21-3p compared with that in the mimic NC group, but pcDNA3.1-FOXO3a displayed no significant effect on the expression of miR-21-3p compared with pcDNA3.1 (Fig. 4A). In addition, pcDNA3.1-FOXO3a transfection significantly increased the expression of FOXO3a compared with that in the pcDNA3.1 group, whereas miR-21-3p mimic significantly downregulated the expression of FOXO3a compared with that in the mimic NC group. Moreover, miR-21-3p mimic significantly inhibited FOXO3a overexpression-induced upregulation of FOXO3a expression in A549 and NCI-H460 cells at both the mRNA and protein level (Fig. 4B and C).

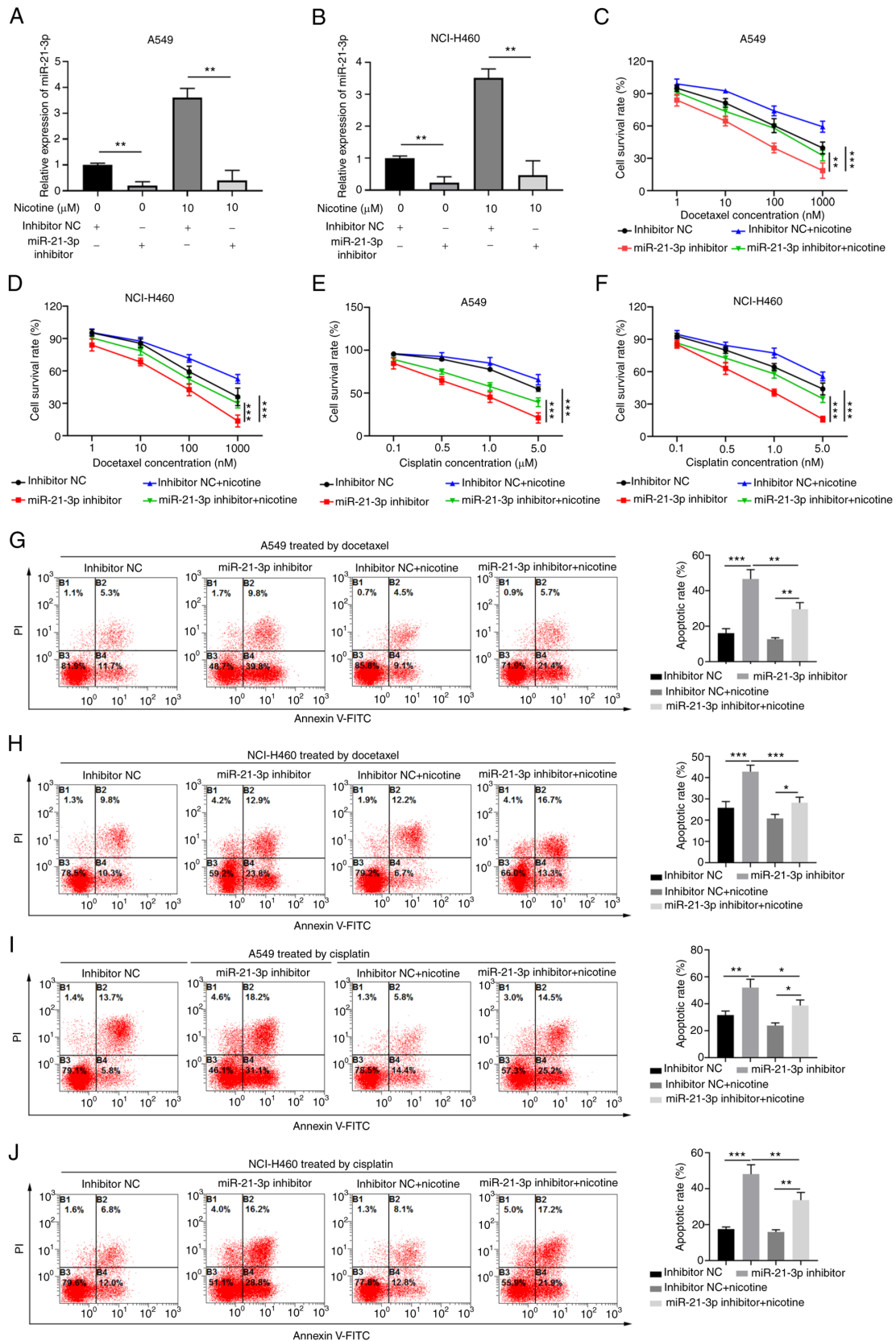


Figure 2. miR-21-3p knockdown sensitizes lung cancer cells to docetaxel or cisplatin treatment. (A) A549 or (B) NCI-H460 cells were transfected with inhibitor NC or miR-21-3p inhibitor, with or without 10 μ M nicotine treatment for 24 h. miR-21-3p expression was analyzed by reverse transcription-quantitative PCR (n=3). (C) A549 or (D) NCI-H460 cell proliferation following transfection with inhibitor NC or miR-21-3p inhibitor, and treatment with different concentrations of docetaxel (1, 10, 100 or 1,000 nM) and nicotine (10 μ M) for 24 h (n=3). (E) A549 or (F) NCI-H460 cell proliferation following transfection with inhibitor NC or miR-21-3p inhibitor, and treatment with different concentrations of cisplatin (0.1, 0.5, 1.0 or 5.0 μ M) and nicotine (10 μ M) for 24 h (n=3). (G) A549 or (H) NCI-H460 cell apoptosis following transfection with inhibitor NC or miR-21-3p inhibitor, and treatment with different concentrations of docetaxel (1, 10, 100 or 1,000 nM) and nicotine (10 μ M) for 24 h (n=3). (I) A549 or (J) NCI-H460 cell apoptosis following transfection with inhibitor NC or miR-21-3p inhibitor, and treatment with different concentrations of cisplatin (0.1, 0.5, 1.0 or 5.0 μ M) and nicotine (10 μ M) for 24 h (n=3). Data are presented as the mean \pm SD. *P<0.05, **P<0.01 and ***P<0.001. miR, microRNA; NC, negative control.

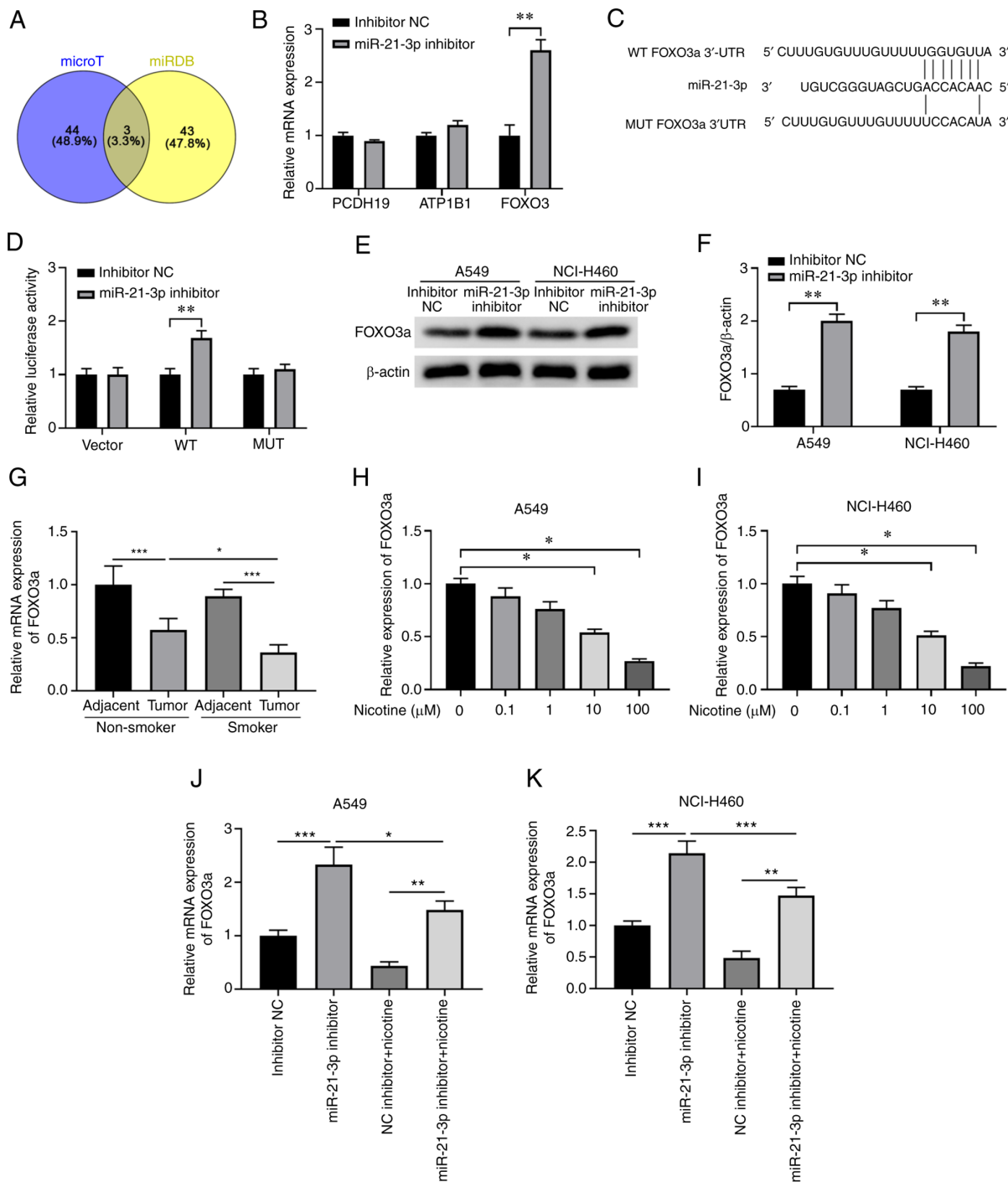


Figure 3. miR-21-3p negatively regulates FOXO3a expression by binding to the 3'-UTR of FOXO3a. (A) Bioinformatics analysis was performed using microT and miRDB databases to predict the potential targets of miR-21-3p. (B) A549 cells were transfected with miR-21-3p inhibitor or inhibitor NC. At 48 h post-transfection, PCDH19, ATP1B1 or FOXO3a expression levels were analyzed by RT-qPCR (n=3). (C) Bioinformatics analysis predicted the potential binding between miR-21-3p and the WT or MUT 3'-UTR of FOXO3a. (D) A549 cells were co-transfected with a control vector, WT 3'-UTR luciferase reporter vector or MUT 3'-UTR luciferase reporter vector and miR-21-3p inhibitor or inhibitor NC. At 48 h post-transfection, relative luciferase activity was analyzed (n=3). A549 or NCI-H460 cells were transfected with inhibitor NC or miR-21-3p inhibitor. At 48 h post-transfection, FOXO3a protein expression levels were (E) determined by western blotting and (F) semi-quantified (n=3). (G) FOXO3a expression in lung cancer tissues from patients with or without consistent nicotine consumption were determined by RT-qPCR (n=5). (H) A549 or (I) NCI-H460 cells were treated with different concentration of nicotine (0, 0.1, 1, 10 or 100 μ M) for 24 h, and the relative expression of FOXO3a was analyzed by RT-qPCR (n=3). (J) A549 or (K) NCI-H460 cells were transfected with miR-21-3p inhibitor and treated with or without nicotine (10 μ M) followed by determination of FOXO3a expression using RT-qPCR (n=3). Data are presented as the mean \pm SD. *P<0.05, **P<0.01 and ***P<0.001. miR, microRNA; UTR, untranslated region; miRDB, microRNA Database; NC, negative control; PCDH19, protocadherin 19; ATP1B1, ATPase Na⁺/K⁺ transporting subunit β 1; RT-qPCR, reverse transcription-quantitative PCR; WT, wild-type; MUT, mutated.

Functionally, compared with that in the pcDNA3.1 group, FOXO3a overexpression significantly suppressed the proliferation of A549 and NCI-H460 cells treated with docetaxel

or cisplatin, whereas miR-21-3p mimic significantly increased the proliferation of A549 and NCI-H460 cells treated with docetaxel or cisplatin compared with that in the mimic NC

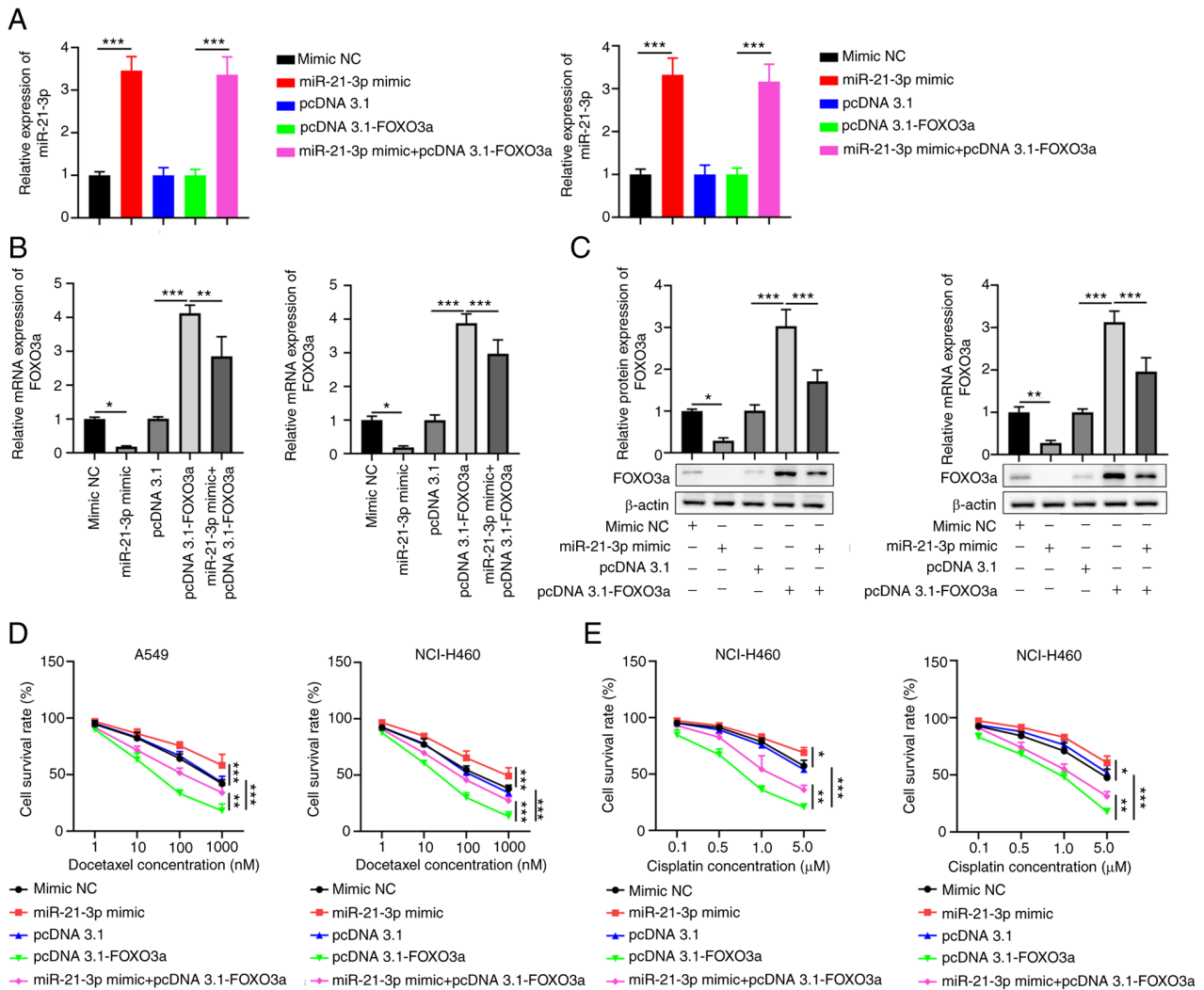


Figure 4. FOXO3a suppresses cell proliferation in lung cancer cells treated with docetaxel or cisplatin, which was reversed by miR-21-3p mimic. A549 or NCI-H460 cells were transfected with pcDNA3.1-FOXO3a, miR-21-3p mimic or the corresponding NCs. At 48 h post-transfection, (A) miR-21-3p, (B) FOXO3a mRNA and (C) FOXO3a protein expression were analyzed (n=3). (D) Cells were cultured with 100 nM docetaxel and then cell proliferation was analyzed by performing CCK-8 assays (n=3). (E) Cells were cultured with 1 μ M cisplatin and then cell proliferation was analyzed by performing CCK-8 assays (n=3). Data are presented as the mean \pm SD. *P<0.05, **P<0.01 and ***P<0.001. miR, microRNA; NC, negative control; CCK-8, Cell Counting Kit-8.

group (Fig. 4C and D). However, miR-21-3p overexpression abrogated the inhibitory effect of FOXO3a overexpression on cell proliferation (Fig. 4C and D). Moreover, FOXO3a overexpression significantly promoted cell apoptosis in lung cancer cells treated with docetaxel or cisplatin compared with that in the pcDNA3.1 group, whereas miR-21-3p mimic significantly decreased cell apoptosis compared with that in the mimic NC group. In addition, miR-21-3p mimic significantly inhibited the promoting effect of FOXO3a overexpression on cell apoptosis in A549 and NCI-H460 cells treated with docetaxel or cisplatin (Fig. 5A-D). Overall, these results suggested that miR-21-3p might promote the chemoresistance of lung cancer cells via negatively regulating FOXO3a.

miR-21-3p promotes chemoresistance in xenograft lung cancer via negatively regulating FOXO3a in vivo. The functional effects of FOXO3a or miR-21-3p overexpression on the chemoresistance of lung cancer cells were investigated *in vivo*. A549 cells were transfected with pcDNA3.1-NC, pcDNA3.1-FOXO3a or pcDNA3.1-FOXO3a + miR21-3p

mimic. Stable transfected cells were implanted into nude mice to establish the lung cancer xenograft tumor model. Following treatment with docetaxel, the FOXO3a overexpression group displayed the smallest tumor size with significantly decreased tumor volumes at 17 days compared with those in the pcDNA3.1 group, whereas miR-21-3p overexpression abrogated this inhibitory effect of FOXO3a overexpression (Fig. 6A-C). Similar results were obtained for the xenograft tumors treated with cisplatin (Fig. 6D-F). The mRNA expression level of FOXO3a was significantly enhanced in the pcDNA3.1-FOXO3a group compared with that in the pcDNA3.1 group, but significantly downregulated in the pcDNA3.1-FOXO3a + miR21-3p mimic group compared with that in the pcDNA3.1-FOXO3a group (Fig. 6G). Moreover, immunohistochemical staining revealed that FOXO3a overexpression significantly decreased the expression of the proliferation marker Ki-67 compared with that in the pcDNA3.1 group, and miR-21-3p mimic rescued Ki-67 expression in the pcDNA3.1-FOXO3a + miR21-3p mimic group (Fig. 6H). Consistent with the *in vitro* results, these results demonstrated that miR-21-3p promoted chemoresistance

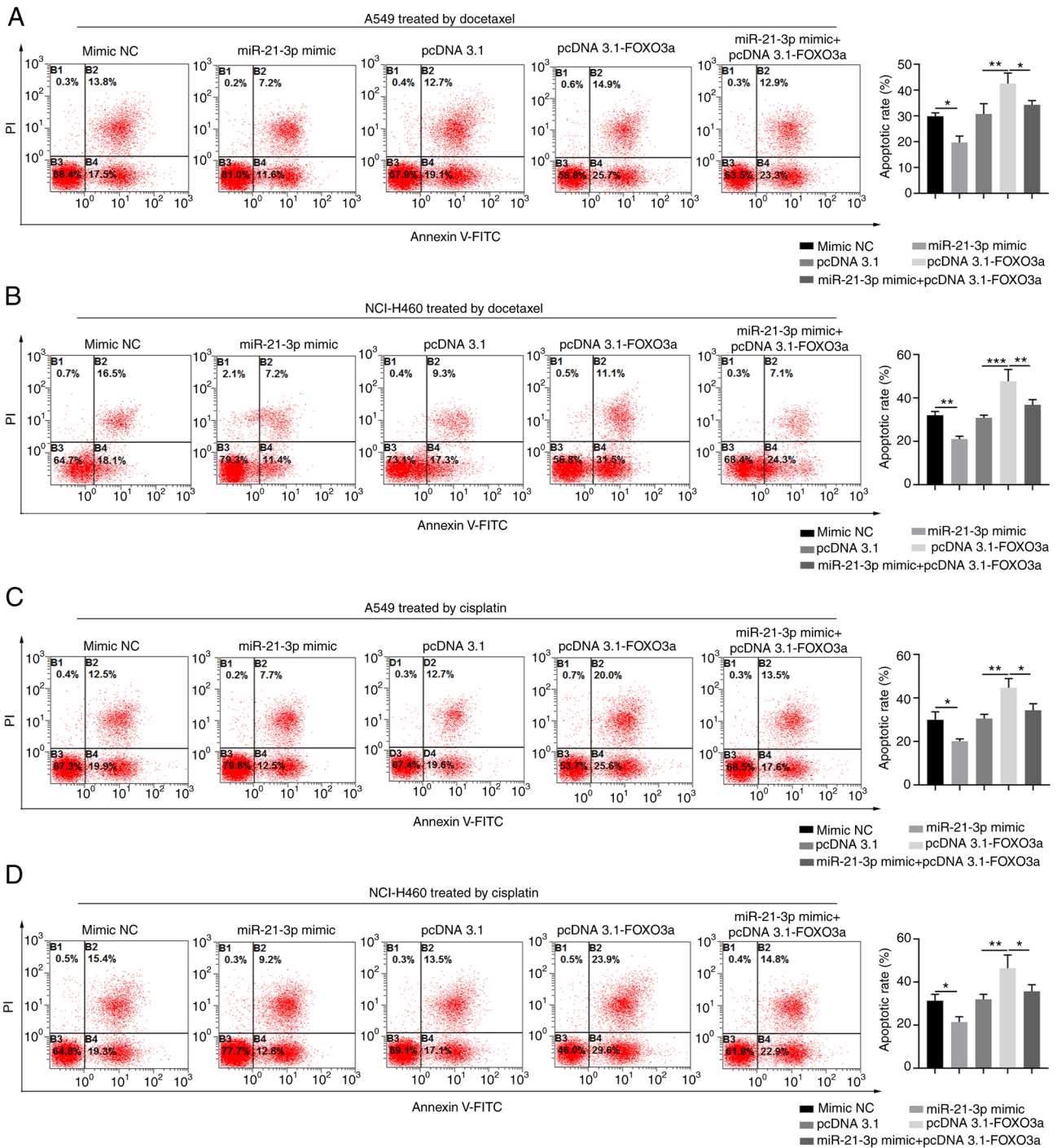


Figure 5. FOXO3a overexpression antagonizes the regulatory function of miR-21-3p in lung cancer cell apoptosis *in vitro*. A549 or NCI-H460 cells were transfected with pcDNA3.1-FOXO3a, miR-21-3p mimic or the corresponding NCs. (A) A549 and (B) NCI-H460 cells were treated with 100 nM docetaxel for 24 h and then cell apoptosis was analyzed by Annexin V/PI staining (n=3). (C) A549 and (D) NCI-H460 cells were treated with 1 μM cisplatin for 24 h and then cell apoptosis was analyzed by Annexin V/PI staining (n=3). Data are presented as the mean ± SD. *P<0.05, **P<0.01 and ***P<0.001. miR, microRNA; NC, negative control.

in xenograft lung cancer via negatively regulating FOXO3a *in vivo*.

Discussion

Lung cancer is the leading cause of cancer-related death worldwide (25). Multiple pharmacogenomic molecular alterations can lead to chemoresistance in lung cancer cells, such as the augmented expression of tubulin III, stathmin, and

ribonucleotide reductase, and the uridine diphosphate glucuronosyltransferase isoform 1A1 genotype is associated with the treatment failure of irinotecan (26-28). It has been found that nicotine can induce resistance to chemotherapy and radiation in a number of tumors by activating a range of intracellular signaling pathways and promoting angiogenesis (29,30). This can cause an additional challenge in managing patients with cancer that have a history of smoking, thus improving the understanding of the pathogenesis involved is critical for the

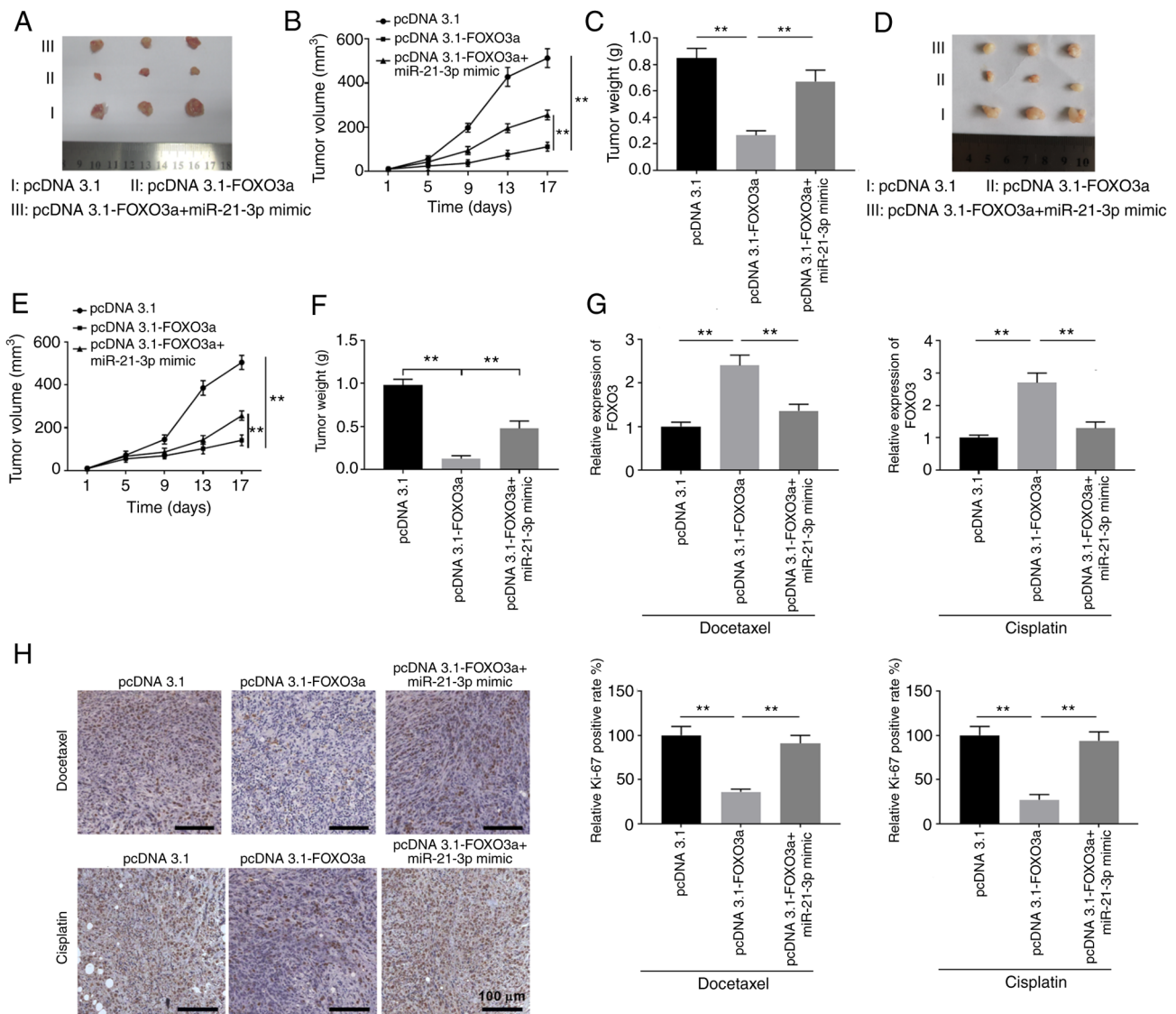


Figure 6. miR-21-3p promotes chemoresistance in xenograft lung cancer via negatively regulating FOXO3a. A549 cells were transfected with pcDNA3.1, pcDNA3.1-FOXO3a or pcDNA3.1-FOXO3a + miR-21-3p mimic. Stable transfected cells were implanted into the nude mice to establish the xenograft tumor model. Subsequently, mice were intraperitoneally injected with nicotine (0.25 mg/kg body weight) every 3 days. (A) Mice were intraperitoneally injected with 5 mg/kg docetaxel every 7 days and (B) the tumor volumes were monitored (n=3). (C) Mice were sacrificed at day 17, and the tumor weight was analyzed (n=3). (D) Mice were intraperitoneally injected with 5 mg/kg cisplatin every 7 days and (E) the tumor volumes were monitored (n=3). (F) Mice were sacrificed at day 17 and the tumor weight was analyzed (n=3). (G) FOXO3a mRNA expression in xenograft tumors was analyzed by reverse transcription-quantitative PCR (n=3). (H) Immunohistochemical staining of Ki-67 was performed in xenograft tumor sections (n=3). Data are presented as the mean \pm SD. **P<0.01. miR, microRNA.

improvement of clinical outcomes. The results of the present study demonstrated that nicotine upregulated miR-21-3p in lung cancer cells, leading to suppression of the proapoptotic protein FOXO3a and subsequent proliferation of tumor cells, therefore resulting in chemoresistance.

miRNAs are small non-coding RNAs that are ~20 nucleotides in length and display extensive post-transcriptional regulatory functions in gene expression involved in various physiological and pathogenic processes (31). For example, miR-21, one of the most frequently upregulated miRNAs in tumors, targets a handful of tumor suppressors, including Bcl-2, PTEN and tumor suppressor P53 (32-34). The dysregulation of miR-21 is associated with a wide variety of hemopoietic and solid neoplasms (35). Previous studies have shown increased miR-21 expression due to exposure to

smoking or nicotine (24,36,37). In particular, the increased levels of plasma miR-21 in patients with lung cancer imply that circulating miR-21 can serve as a diagnostic biomarker that can be used in liquid biopsy (38). Using a cell culture model, Dino *et al* (37) demonstrated that cigarette smoke extract induced the expression of miR-21 in colon cancer cells and promoted tumor invasiveness. In the present study, a five-fold increase in miR-21-3p expression was observed following stimulation with 100 μ M nicotine, indicating that nicotine might induce oncogenic miRNAs, which may serve a role in nicotine-mediated oncogenesis and therapy resistance. The results also implied that miR-21 may serve as a therapeutic target for manipulating chemoresistant lung cancer.

FOXO3a is a transcription factor with a distinct forkhead DNA binding domain (39). As a tumor suppressor, FOXO3a

triggers apoptosis by upregulating the Bcl-2-like protein 11 and p53 upregulated modulator of apoptosis genes, and down-regulating the FLICE-like inhibitory protein gene (40,41). FOXO3a also protects cells from oxidative stress by increasing antioxidants, such as catalase and manganese-containing superoxide dismutase (42). FOXO3a is finely tuned by a miRNA network. For example, FOXO3a is negatively regulated by miR-155 in ischemic renal diseases and some types of cancer (43); by miR-132, miR-212 and miR-223 in inflammatory bowel disease (44); by miR-27a in glioblastoma cells (45); by miR-132 and miR-212 in Alzheimer's disease, leading to neuronal apoptosis (46); and by miR-205 in lung cancer cells (47). A number of *in vitro* and *in vivo* studies have shown promising results of FOX3a-targeting cancer therapy for lung cancer (48-50). Interestingly, cordycepin triggers the re-localization of FOXO3a protein from the nucleus to the cytoplasm in lung cancer cells (51). Moreover, miR-21-3p over-expression could regulate FOXO3a expression to modulate the expression of miR-34b/c in breast cancer (52). In contrast to the available results in the literature, the results of the present study demonstrated FOXO3a downregulation by miR-21-3p via the direct targeting of the FOXO3a 3'-UTR in lung cancer cells, which suggested a novel regulatory mechanism underlying FOXO3a expression.

However, the present study had some limitations. First, due to the deficiency of the clinical samples, correlations between the expression of miR-21-3p or FOXO3a and prognosis of patients with lung cancer with or without nicotine consumption were not further evaluated in the present study. Moreover, the diagnostic and prognostic values of miR-21-3p or FOXO3a in patients with chemoresistant lung cancer require further evaluation. Although the present study demonstrated that nicotine regulated the miR-21-3p/FOXO3a axis to modulate the chemoresistance of lung cancer, the further underlying mechanisms and signaling pathways should be investigated in future studies. Despite these limitations, the present study provided new insights into the role of nicotine in chemoresistant lung cancer.

In summary, the present study identified a molecular mechanism underlying nicotine-mediated chemoresistance in lung cancer by upregulating miR-21-3p expression, which downregulated FOXO3a, leading to tumor cell survival. Collectively, the results suggested that the miR-21-3p/FOXO3a axis may serve as a potential therapeutic target to improve the treatment of chemoresistant lung cancer.

Acknowledgements

Not applicable.

Funding

The present study was supported by the Key Research and Development Project of Shaanxi Province (grant no. 2018SF-065).

Availability of data and materials

The datasets used and/or analyzed during the current study are available from the corresponding author upon reasonable request.

Authors' contributions

SMY conceived and designed the experiments. YQZ and RLC performed the experiments. RLC and LQS analyzed and interpreted the data. YQZ wrote the manuscript. SMY revised the manuscript. SMY and YQZ confirm the authenticity of all the raw data. All authors read and approved the final manuscript.

Ethics approval and consent to participate

The patient studies performed in the present study were approved by the Medical Ethics Committee of Shaanxi Provincial People's Hospital (approval no. SXRMY-2019-024; Xi'an, China) and the animal experiments performed in the present study were approved by the Institutional Review Board of Shaanxi Provincial People's Hospital (approval no. XJTULAC20181428; Xi'an, China).

Patient consent for publication

Not applicable.

Competing interests

The authors declare that they have no competing interests.

References

1. Florou AN, Gkiozos IC, Tsagouli SK, Souliotis KN and Syrigos KN: Clinical significance of smoking cessation in subjects with cancer: A 30-year review. *Respir Care* 59: 1924-1936, 2014.
2. Condoluci A, Mazzara C, Zoccoli A, Pezzuto A and Tonini G: Impact of smoking on lung cancer treatment effectiveness: A review. *Future Oncol* 12: 2149-2161, 2016.
3. Hecht SS: Cigarette smoking: Cancer risks, carcinogens, and mechanisms. *Langenbecks Arch Surg* 391: 603-613, 2006.
4. Hecht SS: Cigarette smoking and lung cancer: Chemical mechanisms and approaches to prevention. *Lancet Oncol* 3: 461-469, 2002.
5. McCann MF, Irwin DE, Walton LA, Hulka BS, Morton JL and Axelrad CM: Nicotine and cotinine in the cervical mucus of smokers, passive smokers, and nonsmokers. *Cancer Epidemiol Biomarkers Prev* 1: 125-129, 1992.
6. Chand HS, Muthumalage T, Maziak W and Rahman I: Pulmonary toxicity and the pathophysiology of electronic cigarette, or vaping product, use associated lung injury. *Front Pharmacol* 10: 1619, 2020.
7. Bracken-Clarke D, Kapoor D, Baird AM, Buchanan PJ, Gately K, Cuffe S and Finn SP: Vaping and lung cancer-a review of current data and recommendations. *Lung Cancer* 153: 11-20, 2021.
8. Beane J, Sebastiani P, Liu G, Brody JS, Lenburg ME and Spira A: Reversible and permanent effects of tobacco smoke exposure on airway epithelial gene expression. *Genome Biol* 8: R201, 2007.
9. Spira A, Beane J, Shah V, Liu G, Schembri F, Yang X, Palma J and Brody JS: Effects of cigarette smoke on the human airway epithelial cell transcriptome. *Proc Natl Acad Sci USA* 101: 10143-10148, 2004.
10. Wang G, Wang R, Strulovici-Barel Y, Salit J, Staudt MR, Ahmed J, Tilley AE, Yee-Levin J, Hollmann C, Harvey BG, *et al*: Persistence of smoking-induced dysregulation of miRNA expression in the small airway epithelium despite smoking cessation. *PLoS One* 10: e0120824, 2015.
11. Willinger CM, Rong J, Tanriverdi K, Courchesne PL, Huan T, Wasserman GA, Lin H, Dupuis J, Joehanes R, Jones MR, *et al*: MicroRNA signature of cigarette smoking and evidence for a putative causal role of MicroRNAs in smoking-related inflammation and target organ damage. *Circ Cardiovasc Genet* 10: e001678, 2017.
12. Qian Y, Mao ZD, Shi YJ, Liu ZG, Cao Q and Zhang Q: Comprehensive analysis of miRNA-mRNA-lncRNA networks in non-smoking and smoking patients with chronic obstructive pulmonary disease. *Cell Physiol Biochem* 50: 1140-1153, 2018.

13. Solleti SK, Bhattacharya S, Ahmad A, Wang Q, Mereness J, Rangasamy T and Mariani TJ: MicroRNA expression profiling defines the impact of electronic cigarettes on human airway epithelial cells. *Sci Rep* 7: 1081, 2017.
14. McConnell DD, Carr SB and Litofsky NS: Potential effects of nicotine on glioblastoma and chemoradiotherapy: A review. *Expert Rev Neurother* 19: 545-555, 2019.
15. Delitto D, Zhang D, Han S, Black BS, Knowlton AE, Vlada AC, Sarosi GA, Behrns KE, Thomas RM, Lu X, *et al*: Nicotine reduces survival via augmentation of paracrine HGF-MET signaling in the pancreatic cancer microenvironment. *Clin Cancer Res* 22: 1787-1799, 2016.
16. Guha P, Bandyopadhyaya G, Polumuri SK, Chumsri S, Gade P, Kalvakolanu DV and Ahmed H: Nicotine promotes apoptosis resistance of breast cancer cells and enrichment of side population cells with cancer stem cell-like properties via a signaling cascade involving galectin-3, $\alpha 9$ nicotinic acetylcholine receptor and STAT3. *Breast Cancer Res Treat* 145: 5-22, 2014.
17. Liu L, Shi X, Zhao H, Yang M, Wang C, Liao M and Zhao J: Nicotine induces cell survival and chemoresistance by stimulating Mcl-1 phosphorylation and its interaction with Bak in lung cancer. *J Cell Physiol*: Feb 11, 2019 (Epub ahead of print).
18. Yuge K, Kikuchi E, Hagiwara M, Yasumizu Y, Tanaka N, Kosaka T, Miyajima A and Oya M: Nicotine induces tumor growth and chemoresistance through activation of the PI3K/Akt/mTOR pathway in bladder cancer. *Mol Cancer Ther* 14: 2112-2120, 2015.
19. Xin M and Deng X: Nicotine inactivation of the proapoptotic function of Bax through phosphorylation. *J Biol Chem* 280: 10781-10789, 2005.
20. Mai H, May WS, Gao F, Jin Z and Deng X: A functional role for nicotine in Bcl2 phosphorylation and suppression of apoptosis. *J Biol Chem* 278: 1886-1891, 2003.
21. Deng X, Liu Z, Liu X, Fu Q, Deng T, Lu J, Liu Y, Liang Z, Jiang Q, Cheng C and Fang W: miR-296-3p negatively regulated by nicotine stimulates cytoplasmic translocation of c-Myc via MK2 to suppress chemotherapy resistance. *Mol Ther* 26: 1066-1081, 2018.
22. Detterbeck FC, Boffa DJ, Kim AW and Tanoue LT: The eight edition lung cancer stage classification. *Chest* 151: 193-203, 2017.
23. Livak KJ and Schmittgen TD: Analysis of relative gene expression data using real-time quantitative PCR and the 2(-Delta Delta C(T)) method. *Methods* 25: 402-408, 2001.
24. Zhang Y, Pan T, Zhong X and Cheng C: Nicotine upregulates microRNA-21 and promotes TGF- β -dependent epithelial-mesenchymal transition of esophageal cancer cells. *Tumour Biol* 35: 7063-7072, 2014.
25. Bade BC and Dela Cruz CS: Lung cancer 2020: Epidemiology, etiology, and prevention. *Clin Chest Med* 41: 1-24, 2020.
26. Li N, Mai Y, Liu Q, Gou G and Yang J: Docetaxel-loaded D- α -tocopheryl polyethylene glycol-1000 succinate liposomes improve lung cancer chemotherapy and reverse multidrug resistance. *Drug Deliv Transl Res* 11: 131-141, 2021.
27. Zhou J, Li Z, Li J, Gao B and Song W: Chemotherapy resistance molecular mechanism in small cell lung cancer. *Curr Mol Med* 19: 157-163, 2019.
28. Takano M and Sugiyama T: UGT1A1 polymorphisms in cancer: Impact on irinotecan treatment. *Pharmgenomics Pers Med* 10: 61-68, 2017.
29. Shen T, Le W, Yee A, Kamdar O, Hwang PH and Upadhyay D: Nicotine induces resistance to chemotherapy in nasal epithelial cancer. *Am J Rhinol Allergy* 24: e73-e77, 2010.
30. Zhang J, Kamdar O, Le W, Rosen GD and Upadhyay D: Nicotine induces resistance to chemotherapy by modulating mitochondrial signaling in lung cancer. *Am J Respir Cell Mol Biol* 40: 135-146, 2009.
31. Huang Y, Shen XJ, Zou Q, Wang SP, Tang SM and Zhang GZ: Biological functions of microRNAs: A review. *J Physiol Biochem* 67: 129-139, 2011.
32. Liu P, Liang H, Xia Q, Li P, Kong H, Lei P, Wang S and Tu Z: Resveratrol induces apoptosis of pancreatic cancer cells by inhibiting miR-21 regulation of BCL-2 expression. *Clin Transl Oncol* 15: 741-746, 2013.
33. Meng F, Henson R, Wehbe-Janek H, Ghoshal K, Jacob ST and Patel T: MicroRNA-21 regulates expression of the PTEN tumor suppressor gene in human hepatocellular cancer. *Gastroenterology* 133: 647-658, 2007.
34. Papagiannakopoulos T, Shapiro A and Kosik KS: MicroRNA-21 targets a network of key tumor-suppressive pathways in glioblastoma cells. *Cancer Res* 68: 8164-8172, 2008.
35. Krichevsky AM and Gabriely G: miR-21: A small multi-faceted RNA. *J Cell Mol Med* 13: 39-53, 2009.
36. Zhu J, Liui B, Wang Z, Wang D, Ni H, Zhang L and Wang Y: Exosomes from nicotine-stimulated macrophages accelerate atherosclerosis through miR-21-3p/PTEN-mediated VSMC migration and proliferation. *Theranostics* 9: 6901-6919, 2019.
37. Dino P, D'Anna C, Sangiorgi C, Di Sano C, Di Vincenzo S, Ferraro M and Pace E: Cigarette smoke extract modulates E-Cadherin, Claudin-1 and miR-21 and promotes cancer invasiveness in human colorectal adenocarcinoma cells. *Toxicol Lett* 317: 102-109, 2019.
38. Wang W, Ding M, Duan X, Feng X, Wang P, Jiang Q, Cheng Z, Zhang W, Yu S, Yao W, *et al*: Diagnostic value of plasma MicroRNAs for lung cancer using support vector machine model. *J Cancer* 10: 5090-5098, 2019.
39. Liu Y, Ao X, Ding W, Ponnusamy M, Wu W, Hao X, Yu W, Wang Y, Li P and Wang J: Critical role of FOXO3a in carcinogenesis. *Mol Cancer* 17: 104, 2018.
40. Dudgeon C, Wang P, Sun X, Peng R, Sun Q, Yu J and Zhang L: PUMA induction by FoxO3a mediates the anticancer activities of the broad-range kinase inhibitor UCN-01. *Mol Cancer Ther* 9: 2893-2902, 2010.
41. Lim EJ, Park DW, Lee JG, Lee CH, Bae YS, Hwang YC, Jeong JW, Chin BR and Baek SH: Toll-like receptor 9-mediated inhibition of apoptosis occurs through suppression of FoxO3a activity and induction of FLIP expression. *Exp Mol Med* 42: 712-720, 2010.
42. Sundaresan NR, Gupta M, Kim G, Rajamohan SB, Isbatan A and Gupta MP: Sirt3 blocks the cardiac hypertrophic response by augmenting Foxo3a-dependent antioxidant defense mechanisms in mice. *J Clin Invest* 119: 2758-2771, 2009.
43. Yamamoto M, Kondo E, Takeuchi M, Harashima A, Otani T, Tsuji-Takayama K, Yamasaki F, Kumon H, Kibata M and Nakamura S: miR-155, a modulator of FOXO3a protein expression, is underexpressed and cannot be upregulated by stimulation of HOZOT, a line of multifunctional treg. *PLoS One* 6: e16841, 2011.
44. Kim HY, Kwon HY, Ha Thi HT, Lee HJ, Kim GI, Hahm KB and Hong S: MicroRNA-132 and microRNA-223 control positive feedback circuit by regulating FOXO3a in inflammatory bowel disease. *J Gastroenterol Hepatol* 31: 1727-1735, 2016.
45. Ge YF, Sun J, Jin CJ, Cao BQ, Jiang ZF and Shao JF: AntagomiR-27a targets FOXO3a in glioblastoma and suppresses U87 cell growth in vitro and in vivo. *Asian Pac J Cancer Prev* 14: 963-968, 2013.
46. Wong HK, Veremeyko T, Patel N, Lemere CA, Walsh DM, Esau C, Vanderburg C and Krichevsky AM: De-repression of FOXO3a death axis by microRNA-132 and -212 causes neuronal apoptosis in Alzheimer's disease. *Hum Mol Genet* 22: 3077-3092, 2013.
47. Cai J, Fang L, Huang Y, Li R, Yuan J, Yang Y, Zhu X, Chen B, Wu J and Li M: miR-205 targets PTEN and PHLPP2 to augment AKT signaling and drive malignant phenotypes in non-small cell lung cancer. *Cancer Res* 73: 5402-5415, 2013.
48. Guo Y, Zhao Y, Zhou Y, Tang X, Li Z and Wang X: LZ-101, a novel derivative of danofloxacin, induces mitochondrial apoptosis by stabilizing FOXO3a via blocking autophagy flux in NSCLC cells. *Cell Death Dis* 10: 484, 2019.
49. Wang J, Sun T, Meng Z, Wang L, Li M, Chen J, Qin T, Yu J, Zhang M, Bie Z, *et al*: XPO1 inhibition synergizes with PARP1 inhibition in small cell lung cancer by targeting nuclear transport of FOXO3a. *Cancer Lett* 503: 197-212, 2021.
50. Gong Q, Cao X, Cao J, Yang X and Zeng W: Casticin suppresses the carcinogenesis of small cell lung cancer H446 cells through activation of AMPK/FoxO3a signaling. *Oncol Rep* 40: 1401-1410, 2018.
51. Joo JC, Hwang JH, Jo E, Kim YR, Kim DJ, Lee KB, Park SJ and Jang IS: Cordycepin induces apoptosis by caveolin-1-mediated JNK regulation of Foxo3a in human lung adenocarcinoma. *Oncotarget* 8: 12211-12224, 2017.
52. Liu X, Feng J, Tang L, Liao L, Xu Q and Zhu S: The regulation and function of miR-21-FOXO3a-miR-34b/c signaling in breast cancer. *Int J Mol Sci* 16: 3148-3162, 2015.

